Structure of dipolar liquids near charged solid surfaces: A nonlinear theory based on a density functional approach and Monte Carlo simulations

D. Das, S. Senapati, and A. Chandra

Structure of dipolar liquids near charged solid surfaces: A nonlinear theory based on a density functional approach and Monte Carlo simulations

D. Das, S. Senapati, and A. Chandra
Department of Chemistry, Indian Institute of Technology, Kanpur, U.P., India 208016

A nonlinear theory for the calculation of density and polarization of dipolar solvents near charged surfaces is developed by using a density functional approach. The theory is based on a weighted density approximation for the isotropic part of the density and the anisotropic (or dipolar) part is calculated by using a perturbative approach. The theory, however, retains the full nonlinear dependence on the surface charge density or the external field. Explicit numerical results are obtained for different values of the external field. It is found that the number density of the solvent near the surface increases with increasing surface charge density indicating the presence of electrostriction. The polarization is found to increase nonlinearly with the external field and exhibits the presence of dielectric saturation at high field strength. The predictions of the present nonlinear theory are compared with the results of Monte Carlo simulations and a good agreement is found for both the density and polarization near charged surfaces. The present simulations clearly reveal a nonlinear behavior of dipolar molecules in presence of the charged surfaces. Also, the nonlinear effects are found to be especially important for interfacial molecules, in agreement with the predictions of the analytical theory presented here. © *1999 American Institute of Physics.* [S0021-9606(99)50416-9]

I. INTRODUCTION

This paper is concerned with the nonlinear dependence of interfacial solvent structure on surface charge density. Studies of dipolar liquids in the vicinity of charged surfaces are extremely important in electrochemistry, biochemistry and surface science. Examples include polar solvents near charged electrodes, charged membranes or macromolecules where the liquid molecules near surfaces move under the influence of an external electric field generated by the charge density of the surfaces. An understanding of the electric field induced perturbations of spatial and orientational structure of interfacial solvent is crucial in the understanding of many chemical and biochemical processes occuring near charged surfaces.

The modifications of the molecular structure of dipolar solvents near charged surfaces have been a subject of much attention in the recent past, both experimentally and theoretically. Toney *et al.*[1,2] measured the spatial and orientational structure of water molecules near charged silver surfaces. They found that water density near the surface is significantly higher than the bulk density which implies that the hydrogen bonding network is disrupted in the water layer next to the charged surfaces. Also, pronounced orientational structure was found in their experiments. Molecular dynamics (MD) and Monte Carlo (MC) simulations provide powerful methods to investigate structural properties of solvents near charged surfaces. Lee *et al.*[3] carried out MD simulations of Stockmayer liquids confined between two charged surfaces. They found that the height of the first peak of the liquid density profile decreases with increasing charge density. This is contrary to the results of a recent simulation of similar systems.[4] Physically one would expect an increase of

liquid density near a surface with increasing surface charge density because of stronger physisorption. Zhu *et al.*[5] carried out MD simulations of water confined between two charged surfaces. They employed the so-called SPC-FP model of water and the surfaces were considered to be planar and uniformly charged. The water density near charged surfaces were found to be greater than bulk density, in agreement with experimental observations. Also, the charge density of the surfaces was found to modify the hydrogen bond network through alignment of water molecules along the electric field generated by the surface charge density. The structure of water near charged surfaces was also investigated by Xia and Berkowitz.[6] These authors carried out MD simulations of the SPC/E model of water[7] near charged platinum surfaces and found no dramatic increase of water density near the surfaces. Also, no significant disruption of hydrogen bonding near the charged surfaces was found. Clearly, our understanding of the structure of dipolar solvents near charged surfaces is far from complete and a current problem in statistical mechanics is to develop an accurate theory for the structure of dipolar liquids in the vicinity of charged solid surfaces. Water is a complex solvent because of its hydrogen bond network. From a theoretical point of view, dipolar hard spheres[8] near uniformly charged planar walls seem to be a good and simple model by which to investigate the properties of interfacial dipolar solvents.

Theoretical studies of interfacial solvents have been primarily based on integral equation and density functional theory (DFT) approaches. Torrie *et al.*[9,10] studied the structure of dipolar hard spheres near charged walls using reference hypernetted chain (RHNC) approximation. Qualitatively, the results were found to be in agreement with that of

computer simulations. Rickayzen and Grimson[11] applied DFT to the system of dipolar hard spheres near charged walls. They used a linear approximation for the density and incorporated the mean spherical approximation (MSA) (Ref. 12) for dipole–dipole correlations and found a layered structure of the solvent near the surface. Subsequently, Moradi and Rickayzen[13] reported an improved DFT of a dipolar fluid in a uniform field by including an accurate expression for the entropy of the inhomogeneous fluid. Their theory also included the three-particle correlations in the fluid in an approximate manner. The nonuniform solvent density and polarization for a system of weakly polar liquid and weakly charged surfaces were calculated and a good agreement with the simulation results was found. Relevant work on the density profile and orientational ordering of dipolar molecules has also been done by Frodl and Dietrich.[14,15] Another development in DFT is the generalized van der Waals (GvdW) theory introduced by Nordholm and co-workers.[16–22] This is a simple theory based on a generalization of cell theory and van der Waals approximations. At present, the theory exists in two forms: a course-grained theory wherein the entropy is considered to be a local functional and a fine-grained theory where this assumption is removed and the entropy functional is taken to be nonlocal. The GvdW theory has been used extensively to study various properties of simple atomic and molecular fluids in nonuniform environment such as adsorption,[17] solvation force,[18] surface tension,[19] and structure of interfaces.[20–22] The theory has been worked out for hard sphere, Lennard-Jones and dipolar fluids and has been found to give qualitatively sound and semiquantitatively accurate results. Quantitatively, the course grained version has been found to underestimate the nonuniform structure near solid surfaces and its fine-grained version overestimates the range of oscillaroty structure at high density. The GvdW theory has played an important role in providing physical insight into various aspects of interfaces involving atomic and molecular fluids.

Another recent development in the density functional theory is the so-called weighted density approximation (WDA).[23–34] This is a nonperturbative approach in which one assumes that a system with an inhomogeneous density distribution can be locally mapped to a corresponding uniform system with a position dependent effective density. In this approach, either the excess free energy or its functional derivative for the inhomogeneous fluid is approximated by that of the corresponding uniform fluid of a different smoothed average density which is determined from suitable weighted averages of the actual nonuniform density of the system. Two recent weighted density schemes which have been quite successful are due to Tarazona[32] and Ashcroft and co-workers.[33,34] The first approach is based on an evaluation of excess free energy density from the corresponding expression of the uniform system using the effective density and the approach of Ashcroft and co-workers is based on a calculation of first order correlation function of an inhomogeneous system using the correspondindg expression for a uniform system. The density functional approaches using WDA have been quite successful in predicting the structure of neutral inhomogeneous hard sphere fluids and ionic solutions

near solid surfaces and, very recently, have been extended to study dipolar fluids near charged surfaces by Patra and Ghosh.[30] These authors used a weighted density approximation for the hard sphere correlation and the electrostatic contributions were included by using a linearization approximation. Because of the use of the linearization approximation, the number density was found to be independent of the surface charge density and the polarization was found to increase linearly with external field. Their results were compared with the MC results of Moradi and Rickayzen[13] and a reasonably good agreement was found except for the first layer near the surface. We note that the liquids studied in these work are very weakly polar and also the surfaces considered are very weakly charged and in such situations a linearization approximation is expected to work. Recent MD simulations of Stockmayer fluids near moderately charged surfaces have shown an increase of density near the surface with increasing surface charge and a nonlinear dependence of polarization on external field.[4] These observations could not be explained by using a linearized theory. Clearly, there remains a need for an improved theory which goes beyond the linearization approximation and includes the full nonlinear dependence of solvent structure on external fields. Such a nonlinear theory based on weighted density functional approach is developed here for the first time.

In this work, we present an analytical theory of solvent structure and polarization near charged surfaces which includes nonlinear dependence on the external field. The theory is based on a weighted density approximation for the isotropic hard sphere correlation and a perturbative approximation for the anisotropic dipolar contribution to the first order correlation function. Self-consistent equations are derived for the solvent density and polarization. Two different weighted density approximations are used for the calculation of hard sphere correlation contributions: the ones of Tarazona[32] and of Ashcroft and co-workers.[34] The final equations are solved iteratively and results are obtained for both approximations and for different values of the surface charge density. To the best of our knowledge, the WDA of Tarazona is applied here for the first time to investigate interfacial structure of dipolar fluids near charged surfaces. One of the objectives of the present work has been to compare the two weighted density approximations in predicting the interfacial structure of dipolar fluids. The present theory with either of the two weighted density approximations nicely reproduces nonlinear effects such as electrostriction[35,36] and dielectric saturation.[37] The dielectric saturation effect is studied by calculating the average angle that a solvent molecule makes with the direction of the external field and this quantity is found to saturate to the value corresponding to the complete alignment of a solvent dipole along the direction of the external field. We note that such saturation effects could not be obtained by using a linearized theory.

We have also carried out detailed Monte Carlo simulations of a dipolar hard sphere solvent confined between two uniformly charged solid surfaces. The purpose of carrying out the MC simulations was to obtain essentially exact results for solvent density and polarization near charged sur-

faces with which the predictions of the present nonlinear theory could be compared and thus its accuracy could be verified. We have simulated four different systems of varying surface charge density. To the best of our knowledge, the effects of changing surface charge density on interfacial structure of dipolar hard spheres are invstigated for the first time by means of MC simulations. All existing simulations of similar systems were carried out at a fixed surface charge density[13] and, thus, the variation of interfacial solvent structure on surface charge density could not be studied. The simulation results are compared with the predictions of the present nonlinear theory and a good agreement is found for both the density and polarization near charged surfaces. The present simulations clearly reveal a nonlinear behavior of dipolar molecules in the presence of charged surfaces. Also, the nonlinear effects are found to be especially important for interfacial molecules which is in agreement with the theoretical predictions.

The organization of the rest of the paper is as follows. In Sec. II, we present the theory and the Monte carlo simulations are discussed in Sec. III. The numerical results of the theory and simulations are presented in Sec. IV and our conclusions are summarized in Sec. V.

II. THEORY

We consider a solvent consisting of nonpolarizable dipolar molecules which are confined between two charged solid surfaces. The solvent molecules are characterized by the so-called dipolar hard sphere potential where dipolar molecules interact through a short range hard sphere interaction and a long range dipole–dipole interaction potential. The solvent molecules also interact with the two solid surfaces which are considered to be infinite hard walls of uniform charge density σ_c. The total Hamiltonian of the system can be expressed in the form

$$H = \sum_i \frac{p_i^2}{2m} + \sum_i \frac{J_i^2}{2I} + \frac{1}{2} \sum_{i \neq j} u_{hs}(r_{ij})$$
$$- \frac{1}{2} \sum_i \mu_i \cdot \mathbf{E}_i^\mu + U_w, \tag{1}$$

where the first two terms represent the kinetic energy and the remaining terms represent the total configurational energy of the system. In Eq. (1), p_i and J_i are, respectively, the linear and angular momenta of the ith molecule, m and I are the mass and moment of inertia of a solvent molecule. r_{ij} is the distance between two molecules i and j, $u_{hs}(r_{ij})$ is the hard sphere (HS) interaction potential which is equal to ∞ for $r_{ij} < \sigma$ and zero otherwise where σ is the diameter of a solvent molecule. μ_i is the dipole moment vector (of magnitude μ) of particle i and $\mathbf{E}_i^\mu$ is the electric field at molecule i due to all other dipoles in the system. The third and fourth terms constitute the dipolar hard sphere potential. The last term in Eq. (1) arises from the interaction of solvent molecules with the two solid surfaces. We assume that the walls are located at positions z' and z'' along the z-axis and x and y axes are parallel to the surfaces. For this geometry, the wall–solvent

interaction potential can be described as a function of the z-coordinate of particle i (z_i) and its orientation (Ω_i) and U_w can be written as

$$U_w = \sum_i u_w(z_i, \Omega_i) \tag{2}$$

with

$$u_w(z_i, \Omega_i) = u_w'(z_i, \Omega_i) + u_w''(z_i, \Omega_i), \tag{3}$$

where u_w' and u_w'' represent the interaction of particle i with walls located at $z = z'$ and $z = z''$, respectively. Both u_w' and u'' include a short range hard sphere–hard wall interaction and a long range Coulombic interaction. Thus, $u_w'(z_i, \Omega_i)$ can be written as

$$u_w'(z_i, \Omega_i) = u_{hw}(|z_i - z'|) - E'(z_i) \cdot \mu_i, \tag{4}$$

where $u_{hw}(|z - z'|)$ is infinity for $|z - z'| < \sigma/2$ and zero otherwise and $E'(z_i)$ is the electric field produced at z_i by the surface charge of the wall localed at z'. In the present calculations, the wall located at z' is assumed to have a positive charge density (σ_c) and the one at z'' is assumed to have a negative charge density of equal magnitude and $z'' > z'$. This generates a uniform field of magnitude $E = 4\pi\sigma_c$ across the system along the positive z direction.

We denote $\rho(\mathbf{r}, \Omega)$ as the position and orientation dependent number density of dipolar molecules between the two surfaces. In DFT, the grand potential of this system at fixed temperature (T), volume, external field, and chemical potential can be exactly expressed as a functional of the inhomogeneous density distribution

$$\bar{\Omega}[\rho(\mathbf{r}, \Omega)] = F[\rho(\mathbf{r}, \Omega)] + \int d\mathbf{r} d\Omega \rho(\mathbf{r}, \Omega)[u(\mathbf{r}, \Omega) - \bar{\mu}], \tag{5}$$

where $u(\mathbf{r}, \Omega)$ is the external potential and $\bar{\mu}$ is the chemical potential. The intrinsic Helmholtz free energy $F[\rho(\mathbf{r}, \Omega)]$ is a universal functional of density and consists of two components

$$F[\rho(\mathbf{r}, \Omega)] = F^{id}[\rho(\mathbf{r}, \Omega)] + F^{ex}[\rho(\mathbf{r}, \Omega)]. \tag{6}$$

The ideal gas free energy functional $F_{id}[\rho(\mathbf{r}, \Omega)]$ is given by

$$F^{id}[\rho(\mathbf{r}, \Omega)] = \beta^{-1} \int d\mathbf{r} d\Omega \rho(\mathbf{r}, \Omega)\{\ln 4\pi\lambda^3 \rho(\mathbf{r}, \Omega) - 1\}, \tag{7}$$

where $\beta = 1/k_B T$, k_B is the Boltzmann constant, T is temperature, and λ is the thermal de Broglie wavelength. The excess free energy $F^{ex}[\rho(\mathbf{r}, \Omega)]$ includes the contribution from intermolecular interactions. $F^{ex}[\rho(\mathbf{r}, \Omega)]$ defines the direct correlation functions of different order through functional derivatives, the most important ones being the first and second order correlation functions defined by

$$c^{(1)}(\mathbf{r}, \Omega) = -\beta \frac{\delta F^{ex}[\rho]}{\delta \rho(\mathbf{r}, \Omega)}, \tag{8}$$

$$c^{(2)}(\mathbf{r}, \mathbf{r}', \Omega, \Omega') = -\frac{\delta^2 F^{ex}[\rho]}{\delta \rho(\mathbf{r}, \Omega) \delta \rho(\mathbf{r}', \Omega')}. \tag{9}$$

Minimizing the grand potential of Eq. (5) with respect to density and evaluating the chemical potential for the uniform bulk density, one obtains an expression for the equilibrium density of the dipolar fluid between the two surfaces. Since the density variation is only along the perpendicular (z) direction, one can write the following expression for the inhomogeneous density:

$$\rho(z,\Omega) = \frac{\rho_0}{4\pi} \exp[-\beta u(z,\Omega) + c^{(1)}(z,\Omega;[\rho(z,\Omega)])$$
$$- c^{(1)}(\rho_0/4\pi)], \qquad (10)$$

for $\sigma/2 < z < (L-\sigma/2)$ and $\rho(z,\Omega)=0$ otherwise. The application of the density functional method can now proceed by the search for a self-consistent solution of Eq. (10). The above equation is a formally exact relation which, in principle, may be solved for $\rho(z,\Omega)$ if the functional $c^{(1)}$ is known. In practice, however, $c^{(1)}$ is generally unknown for ingomogeneous systems and so must be approximated. The simplest approximation of $c^{(1)}(\mathbf{r},\Omega,[\rho(\mathbf{r},\Omega)])$ of an inhomogeneous system involves a perturbative expansion (to first order) in terms of the density inhomogeneity which makes use of the second order direct correlation function of the corresponding homogeneous system and is given by

$$c^{(1)}(\mathbf{r},\Omega,[\rho(\mathbf{r},\Omega)]) - c^{(1)}(\rho_0/4\pi)$$
$$= \int d\mathbf{r}' d\Omega' \widetilde{c}^{(2)}(\mathbf{r},\mathbf{r}',\Omega,\Omega')(\rho(\mathbf{r}',\Omega') - \rho_0/4\pi), \quad (11)$$

where $\widetilde{c}^{(2)}(\mathbf{r},\mathbf{r}',\Omega,\Omega')$ is the second order direct correlation function of the homogeneous liquid. The z-dependent first order correlation function $c^{(1)}(z,\Omega,[\rho(z,\Omega)])$ can be obtained by integrating Eq. (11) over x and y coordinates. Analytical solutions of the second order direct correlation function for a uniform liquid of dipolar hard spheres are available within mean spherical approximation (MSA) (Ref. 12) and are given by

$$\widetilde{c}^{(2)}(\mathbf{r},\mathbf{r}',\Omega,\Omega') = c^{000}(|\mathbf{r}-\mathbf{r}'|) + c^{110}(|\mathbf{r}-\mathbf{r}'|)\phi^{110}(\Omega,\Omega')$$
$$+ c^{112}(|\mathbf{r}-\mathbf{r}'|)\phi^{112}(\Omega,\Omega',\hat{r}). \qquad (12)$$

Here the angular functions $\phi^{110}(\Omega,\Omega')$ and $\phi^{112}(\Omega,\Omega',\hat{r})$ are given by

$$\phi^{110}(\Omega,\Omega') = \hat{\mu}\cdot\hat{\mu}', \qquad (13)$$

$$\phi^{112}(\Omega,\Omega',\hat{r}) = 3(\hat{\mu}\cdot\hat{r})(\hat{\mu}'\cdot\hat{r}) - (\hat{\mu}\cdot\hat{\mu}'). \qquad (14)$$

Here $\hat{\mu}$ and $\hat{\mu}'$ are the unit vectors along dipole moments of particles located at $\mathbf{r}$ and $\mathbf{r}'$ and $\hat{r}=(\mathbf{r}-\mathbf{r}')/|\mathbf{r}-\mathbf{r}'|$. In Eq. (12), $c^{000}(|\mathbf{r}-\mathbf{r}'|)$ represents the isotropic or hard sphere part and the second and third terms represent the anisotropic or dipolar parts of the direct correlation function. In the MSA, $c^{000}(|\mathbf{r}-\mathbf{r}'|)$ is given by the Percus–Yevick (PY) hard sphere (HS) correlation function,[8,39] i.e.,

$$c^{000}(|\mathbf{r}-\mathbf{r}'|) = c^{(2)}_{PY}(|\mathbf{r}-\mathbf{r}'|) = a + b|\mathbf{r}-\mathbf{r}'| + c|\mathbf{r}-\mathbf{r}'|^3,$$
$$(15)$$

for $|\mathbf{r}-\mathbf{r}'|<\sigma$ and zero otherwise. The coefficients a, b, and c are given by

$$a = -\frac{(1+2\eta)^2}{(1-\eta)^4}, \qquad (16)$$

$$b = 6\eta\frac{(1+\eta/2)^2}{(1-\eta)^4}, \qquad (17)$$

$$c = \tfrac{1}{2}\eta a, \qquad (18)$$

where the packing fraction η is equal to $(\pi/6)\rho_0\sigma^3$, where ρ_0 is the density of the homogeneous (bulk) liquid. The anisotropic parts $c^{110}(|\mathbf{r}-\mathbf{r}'|)$ and $c^{112}(|\mathbf{r}-\mathbf{r}'|)$ are also given in terms of the Percus–Yevick hard sphere correlation functions by the following equations:

$$c^{110}(r,\rho_0) = 2\kappa[c^{(2)}_{PY}(r,2\kappa\rho_0) - c^{(2)}_{PY}(r,-\kappa\rho_0)], \qquad (19)$$

$$c^{112}(r,\rho_0) = c^{(0)112}(r) - \frac{3}{r^3}\int_0^r dr' r'^2 c^{(0)112}(r'), \qquad (20)$$

where

$$c^{(0)112}(r,\rho_0) = \kappa[2c^{(2)}_{PY}(r,2\kappa\rho_0) + c^{(2)}_{PY}(r,-\kappa\rho_0)], \quad (21)$$

and vanishes at $r>\sigma$ where $r=|\mathbf{r}-\mathbf{r}'|$. The quantity κ is determined by the equation

$$\frac{(1+4\kappa\eta)^2}{(1-2\kappa\eta)^4} - \frac{(1-2\kappa\eta)^2}{(1+\kappa\eta)^4} = 3y, \qquad (22)$$

where $3y = 4\pi\beta\rho_0\mu^2/3$.

An alternative to Eq. (11) is to adopt the weighted density approximation (WDA) in which $c^{(1)}(z,\Omega,[\rho(z,\Omega)])$ for the inhomogeneous density is obtained by evaluating the corresponding expression $\widetilde{c}^{(1)}$ for the homogeneous fluid at a smoothed density $\bar{\rho}(z,\Omega)$ which, at each point, is a nonlocal functional of $\rho(z,\Omega)$. Thus, we write

$$c^{(1)}(z,\Omega,[\rho(z,\Omega)]) - c^{(1)}(\rho_0/4\pi)$$
$$= \widetilde{c}^{(1)}(\bar{\rho}(z,\Omega)) - \widetilde{c}^{(1)}(\rho_0/4\pi). \qquad (23)$$

$\bar{\rho}(z,\Omega)$ can be interpreted as the effective density of a locally uniform fluid to which the actual nonuniform fluid is mapped. The basic physical assumption underlying the above approximation is that each particle in the inhomogeneous fluid, through its interactions with the surrounding particles, contributes to the excess free energy as though it interacted with an effective locally uniform medium.

Although the perturbative approximation in Eq. (11) is simpler to deal with, the WDA has been known to provide a better treatment for the isotropic hard sphere correlation contributions.[32–34] Therefore, we decompose the total first order direct correlation function into two parts; $c^{(1)} = c^{(1)}_{hs} + c^{(1)}_{ex}$, where $c^{(1)}_{hs}$ is the isotropic hard sphere contribution to the first order correlation function and $c^{(1)}_{ex}$ represents the remaining anisotropic (or excess) contribution which arises from the explicit dipole–dipole electrostatic interactions and also from the coupling of electrostatic and hard sphere interactions. Following earlier work, we adopt a partially nonperturbative approach in which we evaluate the isotropic hard sphere contribution $c^{(1)}_{hs}$ using the WDA and the remaining anisotropic part $c^{(1)}_{ex}$ through a perturbative approach by us-

ing an equation similar to Eq. (11) but involving only aniso-tropic terms of the second order direct correlation function. The expression for the inhomogeneous density can now be written in the following form:

$$\rho(z,\Omega) = \frac{\rho_{hs}(z)}{4\pi} \exp\left[-\beta u(z,\Omega) + \int dx dy d\mathbf{r}' d\Omega'\right.$$

$$\times [c^{110}(|\mathbf{r}-\mathbf{r}'|;\rho_0)\phi^{110}(\Omega,\Omega') + c^{112}$$

$$\left.\times (|\mathbf{r}-\mathbf{r}'|,\rho_0)\phi^{112}(\Omega,\Omega',\hat{r})](\rho(z',\Omega) - \rho_0/4\pi)\right]$$

(24)

and

$$\rho_{hs}(z) = \rho_0 \exp[c_{hs}^{(1)}(\bar{\rho}_{hs}(z)) - c_{hs}^{(1)}(\rho_0)]. \quad (25)$$

Here $c_{hs}^{(1)}(\bar{\rho}_{hs}(z))$ refers to the hard sphere contribution to the first order correlation function defined through the WDA at an effective density $\bar{\rho}_{hs}(z)$ obtained as the weighted average

$$\bar{\rho}_{hs}(z) = \int dz' \rho_{hs}(z') w(|z-z'|), \quad (26)$$

where $w(z-z')$ is a planar averaged weight function. $\bar{\rho}_{hs}(z)$ can be physically interpreted as the effective hard sphere density to which the actual nonuniform density is locally mapped so that the hard sphere contribution to the one-particle correlation function is correctly reproduced when the expression for the uniform system is evaluated with this density. The calculation of $\bar{\rho}_{hs}(z)$ within two different approximations will be discussed later.

We now expand the position and orientation dependent density $\rho(z,\Omega)$ in the basis set of spherical harmonics $Y_{lm}(\Omega)$ as follows:[38,39]

$$\rho(z,\Omega) = \sum_{lm} a_{lm}(z) Y_{lm}(\Omega). \quad (27)$$

Clearly, the angle averaged number density $\rho(z) = \int d\Omega \rho(z,\Omega) = \sqrt{4\pi} a_{00}(z)$ and the solvent polarization $P(z)$ is related to $a_{10}(z)$ by the following equation:

$$P(z) = \sqrt{\frac{4\pi}{3}} \mu a_{10}(z). \quad (28)$$

It is to be noted that other density components vanish within the present approximation. Substitution of Eq. (27) and explicit forms of angular functions ϕ^{110} and ϕ^{112} into Eq. (24) and carrying out the angular integrations give the following simplified expressions for the density components,

$$a_{00}(z) = \frac{\rho_{hs}(z)}{\sqrt{4\pi}} \frac{\sinh\{\beta E\mu + I_1(z) + I_2(z)\}}{\beta E\mu + I_1(z) + I_2(z)}, \quad (29)$$

$$a_{10}(z) = \left(\frac{3}{4}\right)^{1/2} \rho_{hs}(z) \left[\frac{\cosh\{\beta E\mu + I_1(z) + I_2(z)\}}{\beta E\mu + I_1(z) + I_2(z)}\right.$$

$$\left. - \frac{\sinh\{\beta E\mu + I_1(z) + I_2(z)\}}{(\beta E\mu + I_1(z) + I_2(z))^2}\right]. \quad (30)$$

In Eqs. (29) and (30), $I_1(z)$ and $I_2(z)$ are given by

$$I_1(z) = \int dz' a_{10}(z) c^{110}(z-z'), \quad (31)$$

and

$$I_2(z) = \int dx dy d\mathbf{r}' a_{10}(z') c^{112}(|\mathbf{r}-\mathbf{r}'|) \left(\frac{3|z-z'|^2}{|\mathbf{r}-\mathbf{r}'|^2} - 1\right), \quad (32)$$

where $c^{110}(z-z')$ is obtained from $c^{110}(|\mathbf{r}-\mathbf{r}'|)$ by integrating over x and y coordinates. One can also calculate the quantity $\langle\cos\theta\rangle_z$, the average value of $\cos\theta$ for a solvent molecule at a given value of the position z from the surface. $\langle\cos\theta\rangle_z$ can be written in terms of position and orientation dependent density as

$$\langle\cos\theta\rangle_z = \frac{\int d\Omega \cos\theta \rho(z,\Omega)}{\int d\Omega \rho(z,\Omega)} = L[\beta\mu E + I_1(z) + I_2(z)], \quad (33)$$

where L refers to the Langevin function, defined as $L(x) = \coth(x) - x^{-1}$. The expression for $\langle\cos\theta\rangle_z$ in the above equation includes the effect of dielectric saturation, since $\langle\cos\theta\rangle_z$ in the Langevin form approaches the saturated value of $\cos\theta$ (1 or -1 depending on direction of the external field) at large field strengths.

We note that the nonlinearity of Eq. (24) is retained in Eqs. (29)–(30). Equations (29)–(33) are the key results of this paper which constitute a set of nonlinear equations for the calculation of number density, polarization, and average orientation of a molecule near charged surfaces. We note that when Eqs. (29) and (30) are linearized with respect to the external field, we recover the equations of Ref. 30, where the number density $a_{00}(z)$ is found to be independent of the surface charge density and the polarization is found to increase linearly with the external field. The linearized theory also predicts a linear increase of $\langle\cos\theta\rangle_z$ with electric field and, thus, the dielectric saturation effect as exhibited by Eq. (33) cannot be obtained by using a linearized theory. It will be shown in the next section that nonlinear effects can be significant for surfaces of not too low charge density, in agreement with the results of recent computer simulations.

We now discuss the calculation of the hard sphere density $\rho_{hs}(z)$ which depends on $c_{hs}^{(1)}(z)$ and $w(z-z')$. There are several ways to calculate these quantities. The WDA proposed by Tarazona[32] is based on the construction of an approximate free energy functional which gives correct thermodynamics and nearly correct response function of a homogeneous system and it is expected that the same free energy functional can be successfully used to determine the structure and thermodynamics of inhomogeneous systems by employing a suitably calculated effective density, $\bar{\rho}(z)$. In this scheme, $c_{hs}^{(1)}(z;\bar{\rho}(z))$ is obtained by calculating the hard sphere contribution to the excess free energy density f_{hs}^{ex} [defined through $F_{hs}^{ex} = \int d\mathbf{r}\rho(\mathbf{r})f_{hs}^{ex}(\mathbf{r})$] of the uniform system using the effective density $\bar{\rho}$. The first order correlation function can be obtained through functional differentiation of the excess free energy and is given by

$$c_{hs}^{(1)}(z;\bar{\rho}) = -\beta f_{hs}^{ex}[\bar{\rho}(z)] - \beta \int dz' \rho(z') f'_{hs}^{ex}[\bar{\rho}(z)]$$

$$\times \frac{w(z-z';\bar{\rho}(z'))}{1-\bar{\rho}_1(z') - 2\bar{\rho}_2(z')\bar{\rho}(z')}, \qquad (34)$$

$$c_{hs}^{(1)}[\rho_0] = -\beta f_{hs}^{ex}[\rho_0] - \beta \rho_0 f'_{hs}^{ex}[\rho_0], \qquad (35)$$

where f'_{hs}^{ex} is the derivative of f_{hs}^{ex} where the excess free energy density can be obtained from the well-known and quasiexact Carnaham–Starling equation of state. The expression for the weight function in this approach is given by the second order expansion

$$w(|z-z'|;\bar{\rho}(z)) = w^{(0)}(|z-z'|) + w^{(1)}(|z-z'|)\bar{\rho}(z)$$

$$+ w^{(2)}(|z-z'|)\bar{\rho}(z)^2, \qquad (36)$$

with the density independent component weight functions normalized as $\int dz' w^{(i)}(z-z') = \delta_{i,0}$. The weighted density $\bar{\rho}(z)$ in this scheme can be expressed as

$$\bar{\rho}(z) = \frac{2\bar{\rho}^{(0)}(z)}{[1-\bar{\rho}^{(1)}(z)] + [(1-\bar{\rho}^{(1)}(z))^2 - 4\bar{\rho}^{(0)}(z)\bar{\rho}^{(2)}(z)]^{1/2}}, \qquad (37)$$

where the effective density components $\bar{\rho}^{(i)}(z)$ $(i=0,1,2)$ are defined by

$$\bar{\rho}^{(i)}(z) = \int dz' \rho(z') w^{(i)}(|z-z'|). \qquad (38)$$

Explicit expressions for the density independent component weight functions are available in the literature.[32] In the present work, we refer to the above scheme of Tarazona as Scheme A.

The WDA of Denton and Ashcroft[34] (Scheme B), on the otherhand, specifies the weight function for obtaining $\bar{\rho}$ and to approximate $c_{hs}^{(1)}$. Demanding that the first functional derivative of $c_{hs}^{(1)}$ with respect to density yield the correct two-particle direct correlation function in the uniform limit, one obtains the following explicit expression for the weight function

$$w(\mathbf{r}-\mathbf{r}') = \frac{c_{hs}^{(2)}(|\mathbf{r}-\mathbf{r}'|;\bar{\rho})}{\partial c_{hs}^{(1)}(\bar{\rho})/\partial\bar{\rho}}. \qquad (39)$$

In the approximation of Denton and Ashcroft, one uses the PY solution for $c_{hs}^{(2)}(|\mathbf{r}-\mathbf{r}'|;\bar{\rho})$ and the expression for $c_{hs}^{(1)}$ is given by

$$c_{hs}^{(1)} = -\frac{1}{2}[14\eta - 13\eta^2 + 5\eta^3]/(1-\eta)^3 + \ln(1-\eta). \qquad (40)$$

Schemes A and B provide non-perturbative routes to the calculation of $\rho_{hs}(z)$. Once $\rho_{hs}(z)$ is known, $a_{00}(z)$ and $a_{10}(z)$ are determined by solving nonlinear integral equations as given by Eqs. (29) and (30). These equations are solved iteratively by the standard method of discretization and integration by the trapezoidal rule. In the iteration process, the old profiles $\rho_{hs}(z)$ and $a_{10}(z)$ are used in the right hand side

to get the new ones in the left hand side and the process is repeated until convergence is reached. To obtain convergence, we have used the standard technique of mixing the old solution $(1-\alpha)$ with the new ones (α) during iteration with the help of a mixing parameter α. The value of α is taken to be 0.005 and the process required a few thousand iterations before reaching convergence.

The systems studied here are specified by the values of the following reduced parameters: dipole moment $\mu^* = \sqrt{\mu^2/k_B T\sigma^3}$, electric field (produced by the two surfaces) $E^* = E\sqrt{\sigma^3/k_B T}$ and the bulk density $\rho^* = \rho\sigma^3$. The solvent in the present calculations is characterized by $\mu^* = 1.29$ and $\rho^* = 0.74$. We have, however, used several different values of the reduced electric field from $E^* = 0$ to $E^* = 10$. The separation between the two walls is 9.5σ which is sufficiently large so that the solvation zones at the two surfaces do not overlap and a bulk region of homogeneous density is found in the middle region of all the systems.

III. MONTE CARLO SIMULATIONS

We have carried out Monte Carlo simulations of a dipolar hard sphere fluid confined between two uniformly charged hard walls. The liquid is characterized by the same parameters as were considered in the last section. The simulations were carried out with 256 particles in a rectangular box of dimension $L \times L \times h$, where h is the separation between the walls and L is the length of the central simulation box in x and y directions. Periodic boundary conditions were employed in the x and y directions. The simulations are carried out for four different values of the reduced electric field $E^* = 0$, 2, 4, and 6. For all the systems, the walls are located at $z=0$ and $z=9.5\sigma$ and periodic boundary conditions are set at 0 and 6.136σ along x and y directions. This ensures a bulk region of homogeneous density $\rho^* = 0.74$ in the middle region of all the systems. In the simulations, the long-range dipolar interactions are treated by using the Ewald summation (slab adapted) method.[40] In this method, the slabs of dipolar liquid are separated by a region which contains no dipolar molecules and has a dielectric constant of 1. In the present calculations of the Ewald summation, the periodicity of the systems in the z-direction is 25.5σ which corresponds to having an empty region of 17σ bewteen the slabs of dipolar molecules. We have verified that the surfaces are sufficiently far apart that the interactions between the slabs are negligible. The Ewald parameters employed are: the convergence parameter $\alpha/L = 6.4$, a reciprocal cutoff of $15\sigma^{-1}$ and $\epsilon' = \infty$ where ϵ' is the dielectric constant of the medium which surrounds the infinite array of periodically replicated systems. The minimum image convention was used for the real space portion of the Ewald sum. In the MC simulations, all systems were first equilibrated for 25 000 MC passes and then the simulations were run for another 50 000 MC passes for the calculation of the final averages.

The number density was calculated by computing the average number of molecules in slabs of thickness $\Delta z = 0.02\sigma$. The orientational structure of solvent dipoles are calculated by finding the solvent polarization along the field direction (z) which is obtained by calculating the total dipole
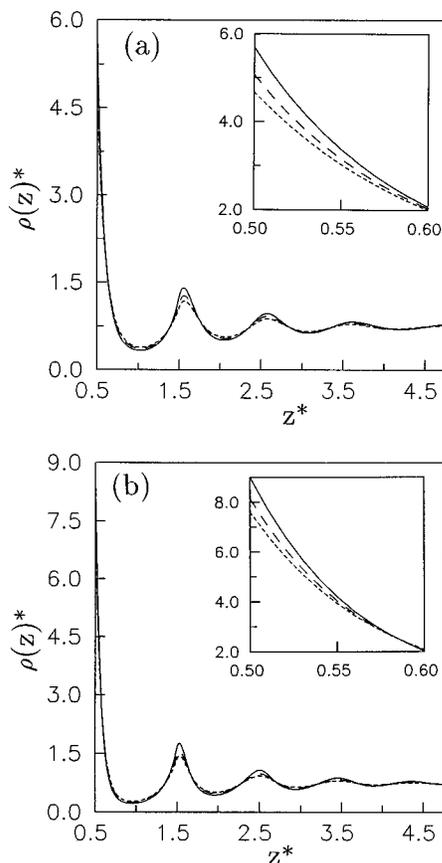
FIG. 1. The variation of solvent density with distance from a charged surface obtained by using (a) Scheme A and (b) Scheme B. The short dashed, long dashed, and solid curves are for $E^*=2$, 4, and 6, respectively. The reduced distance $z^*=z/\sigma$. Other reduced quantities are defined in the text. The insets show the solvent densities near the charged surface.
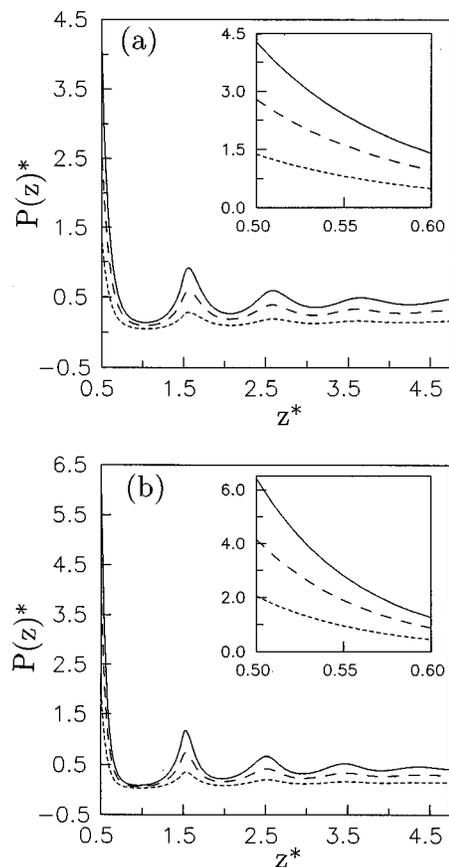

FIG. 2. The variation of solvent polarization with distance from a charged surface obtained by using (a) Scheme A and (b) Scheme B. The short dashed, long dashed, and solid curves are for $E^*=2$, 4, and 6, respectively. The insets show the solvent polarizations near the charged surface.

moment along z-direction in different slabs between the two surfaces. The simulation results of the inhomogeneous density, polarization and average orientation of solvent molecules are presented in the next section.

IV. NUMERICAL RESULTS

We first discuss the predictions of the present theory. In Fig. 1, we have shown the results of $\rho(z)$ for three different values of the reduced electric field E^*. The results of Fig. 1(a) are obtained by using Scheme A for the calculation of $\rho_{hs}(z)$ [Eqs. (26 and (36)] and the ones of Fig. 1(b) correspond to Scheme B [Eq. (39)]. It is seen that the density profiles are highly nonuniform near the walls. Also, the density at the surface increases with increasing external field. This implies that the charge density of the surfaces attracts the solvent molecules and leads to a stronger physisorption at charged surfaces. Although in both cases, an increase of number density near the surface is found with increasing electric field, the contact densities obtained in Scheme B are significantly higher than the corresponding densities obtained by using Scheme A. The increase of solvent density near the surfaces is a measure of the electrostriction caused by the charge density of the surfaces. It is clear from the figures that this increase of interfacial density (or electros-

triction) is rather significant for systems of higher surface charge density. This is a nonlinear effect which cannot be explained by using a linearized theory.

We next discuss the theoretical results of solvent polarization which are shown in Figs. 2(a) (Scheme A) and 2(b) (Scheme B). The solvent polarization is found to be most significant near the surface and then it oscillates until the bulk value is reached. Again, the contact values of the polarization obtained in Scheme B are found to be larger compared to the corresponding results in Scheme A and the results also seem to depend rather strongly on the strength of the applied field. For example, in case of Scheme A, the height of the first peak of the reduced polarization is 1.38 for $E^*=2$, 2.78 for $E^*=4$ and it is 4.27 for $E^*=6$. Clearly, the polarization increases with surface charge density in a nonlinear fashion for the systems studied in this work. The predicted values of the solvent polarization near the surfaces are higher than the corresponding values obtained by linearizing Eqs. (29) and (30). For example, the linearized theory predicts a value of 4.11 for the polarization at surface for $E^*=6$, whereas the present nonlinear theory gives a higher value of 4.27 for the same quantity. This enhancement of polarization is partly due to an enhanced density of solvent molecules or electrostriction near the charged surfaces. Clearly, the electrostriction and polarization effects are coupled with each other. In Fig. 3, we have plotted the quan-
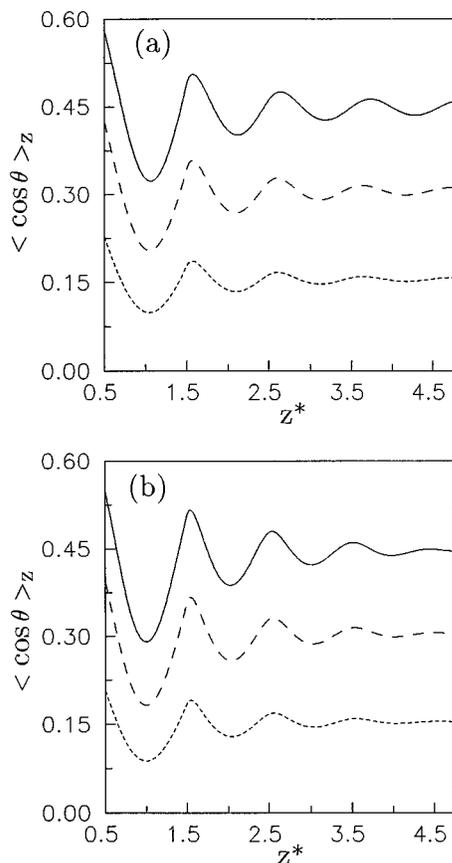
FIG. 3. The variation of $\langle \cos \theta \rangle_z$ with distance from the charged surface obtained by using (a) Scheme A and (b) Scheme B, where θ is the average angle that a solvent molecule makes with the direction of the external field. The short dashed, long dashed, and solid curves are for $E^* = 2$, 4, and 6, respectively.

tity $\langle \cos \theta \rangle_z$ against z for three different values of the external electric field E^*. $\langle \cos \theta \rangle_z$ describes the average orientation of solvent molecules at a distance z from the charged surface located at $z = 0$ and it is unity when the solvent molecules are completely oriented along the electric field. It is clear from Fig. 3 that the solvent molecules near the surface are more oriented than the bulk molecules along the external field. Also, the profiles of $\langle \cos \theta \rangle_z$ are seen to oscillate with distance from the surface which can be attributed to the competing effects of external field and dipole–dipole interactions.

The goal of the present study has been to investigate the importance of nonlinear behavior of dipolar solvents near charged surfaces. Such nonlinear effects are manifested more clearly in the electric field dependence of the increase in number density and average orientation of solvent molecules at interfaces which are shown in Fig. 4. The predictions of the linearized theory of Patra and Ghosh[30] are also shown for comparison. The change in number density is denoted by $\Delta \rho(z)$, where $\Delta \rho(z) = \rho(z;E) - \rho(z;E=0)$. It is clear from Fig. 4(a) that signficant nonzero values of $\Delta \rho(z;E)$ are predicted in the interfacial region by the present theory for $E^* = 4$ and 6 whereas the linearized theory predicts $\Delta \rho(z;E) = 0$ for all values of the external field. Thus, significant electrostriction can occur near charged surfaces contrary to the
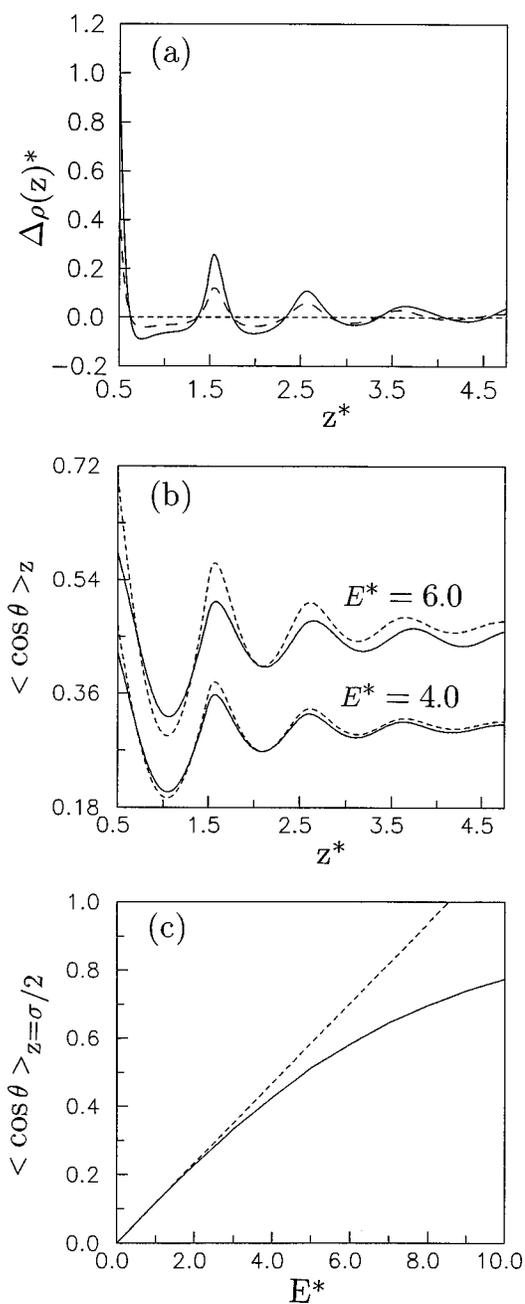

FIG. 4. (a) The variation of change in number density with distance from the charged surface. The long-dashed and solid curves represent the predictions of the present theory for $E^* = 4$ and 6, respectively. The short-dashed curve shows the predictions of the linearized theory (Ref. 26). (b) The variation of $\langle \cos \theta \rangle_z$ with distance for $E^* = 4$ and 6. The solid and dashed curves show, respectively, the predictions of the present nonlinear theory and the linearized theory. (c) The dependence of $\langle \cos \theta \rangle_z$ on the external field. The solid and dashed curves represent, respectively, the predictions of the present nonlinear theory and the linearized theory of Ref. 30. All results are obtained by using Scheme A.

predictions of the linearized theory. We next discuss the nonlinear effects associated with the average orientation of solvent molecules which are shown in Figs. 4(b) and 4(c). In Fig. 4(b), we have compared the profiles of $\langle \cos \theta \rangle_z$ for $E^* = 4$ and 6, as predicted by the present nonlinear theory and by the linarized theory.[30] The linearized theory is found to overestimate the extent of orientation near the charged surfaces. According to the linearized theory, $\langle \cos \theta \rangle_z$ increases

linearly with the electric field E^*, whereas the actual dependence is nonlinear because $\langle \cos \theta \rangle_z$ cannot exceed its saturated value of unity. This nonlinear approach of $< \cos \theta \rangle_z$ to its saturated value of unity is correctly predicted by the present theory which is shown in Fig. 4(c). We also note that, according to the linearized theory, the value of $\langle \cos \theta \rangle_z$ can become higher than 1.0 for large surface charges. This unphysical behavior is corrected by the present nonlinear theory where $\langle \cos \theta \rangle_z$ always remains less than one and it saturates to the value of unity in limit of very high surface charge density.

In Fig. 5, we have compared the predictions of the present theory with the results of MC simulations for the density, polarization, and average orientation of solvent molecules for $E^* = 4$. It is seen that the overall agreement between the theoretical and simulation results is quite good. Quantitatively, the results obtained by using Scheme B (Denton–Ashcroft) is found to overestimate the contact density and polarization to some extent. The agreement is indeed very good when Scheme A is used for the calculation of the number density and the polarization. Both schemes give good results for $\langle \cos \theta \rangle_z$ as can be seen in Fig. 5(c). The higher value of the contact polarization predicted in Scheme B is mainly due to the larger value of contact density predicted in that scheme and this effect is not reflected in $\langle \cos \theta \rangle_z$ which is related to the ratio of the polarization and the density. The nonlinear effects are also observed in simulations as shown in the insets of Figs. 5(a) and 5(c). The density of solvent molecules near a charged surface is found to be higher than that near an uncharged surface which confirms the presence of electrostriction near charged surfaces. Also, the average orientation ($\langle \cos \theta \rangle_z$) of solvent molecules near a charged surface increases nonlinearly with the external field which is in good agreement with the predictions of the present theory.

V. SUMMARY AND CONCLUSIONS

We have presented a nonlinear theory for the calculation of density and polarization of dipolar solvents near charged surfaces by using a density functional approach. The theory is based on a weighted density approximation for the isotropic part of the density and the anisotropic (or dipolar) part is calculated by using a perturbative approach. The theory, however, retains the full nonlinear dependence on the surface charge density or the external field. Two different approaches are employed in the calculation of the isotropic hard sphere part of the inhomogeneous density. The first approach (Scheme A) is due to Tarazona[32] and the second one is due to Denton and Ashcroft.[34] Explicit numerical results are obtained for several different values of the external field (or the surface charge density). We have also carried out Monte Carlo simulations of dipolar hard sphere solvents confined between two surfaces of varying charge density.

We have compared the theoretical predictions of the density and polarization obtained by using Tarazona's approach (Scheme A) and Denton–Ashcroft approach (Scheme B) in the calculation of the hard sphere density. Although the two approaches are found to give qualitatively similar results, the values of contact density and polarization for
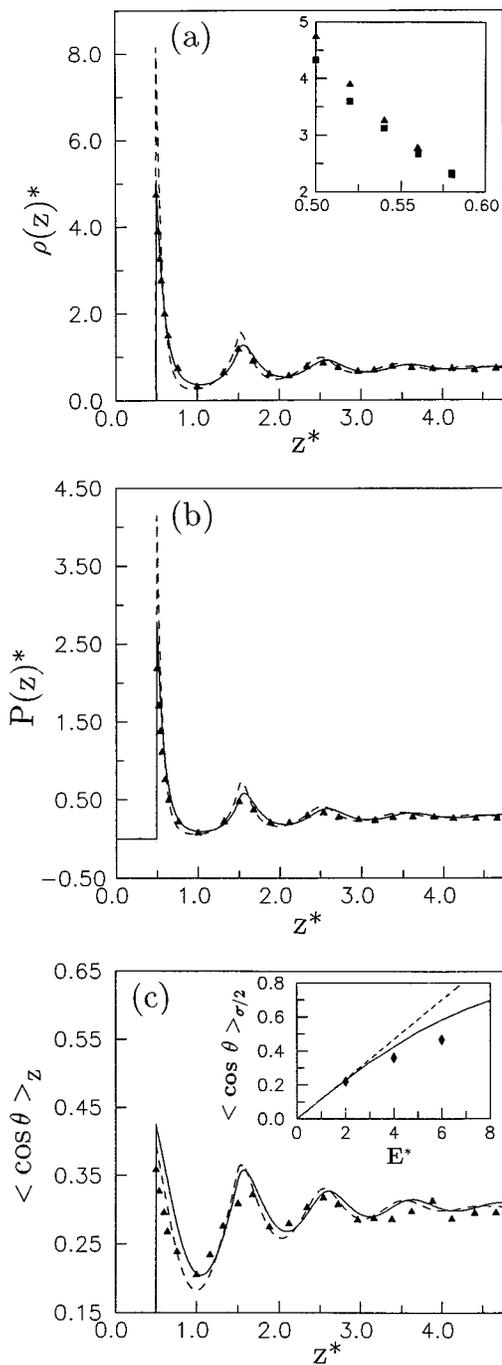

FIG. 5. The comparison of the theoretical and simulaton results of (a) solvent density (b) polarization and (c) average orientation of solvent molecules near the charged surface. The solid and dashed curves represent the results of the present theory for $E^* = 4$ obtained by using Scheme A and Scheme B, respectively, and the solid triangles represent the simulation results for the same external field. The solid squares in the inset of (a) are the simulation results of density for $E^* = 0$. In the inset of (c), the solid diamonds, the solid curve and the dashed curve represent, respectively, the results of simulations, the nonlinear theory (Scheme A) and the linearized theory for the average orientation of molecules at the surface for different values of the external field.

Scheme B are found to be significantly higher than the corresponding results for Scheme A. Comparison with Monte Carlo results show that Tarazona's approach provides better agreement with simulation results. It is found that the number density of the solvent near the surface increases with

increasing surface charge density due to the presence of elec-trostriction. The polarization is found to increase nonlinearly with the external field and to exhibit the presence of dielectric saturation at high field strength. The solvent molecules near the surfaces are found to be more oriented along the field than the bulk molecules which is in agreement with the results of computer simulations. We note that the nonlinear interfacial phenomena such as electrostriction and dielectric saturation could not be explained by using a linearized theory. One requires a nonlinear theory to explain these effects. Such a nonlinear theory for interfaces based on density functional approach is presented here for the first time.

The present theory can be extended in many directions to investigate more complex interfacial systems. For example, it would be interesting to study the structure of mixed dipolar solvents near charged surfaces. Here the interfacial structure is expected to be rather complex because of selective adsoprtion of one species against the other at charged surfaces. Also, it would be interesting to extend the present theory to investigate ionic solutions near charged electrodes where again the interfacial structure can be quite complex when molecularity of both ions and solvent are considered. Work in these directions is in progress.

[1] M. F. Toney, J. N. Howard, J. Richer, G. L. Borges, D. C. Wiesler, D. Yee, and L. B. Sorensen, Nature (London) **368**, 444 (1994).

[2] M. F. Toney, J. N. Howard, J. Richer, G. L. Borges, J. G. Gordon, O. R. Melroy, D. G. Wiesler, D. Yee, and L. B. Sorensen, Surf. Sci. **335**, 326 (1995).

[3] S. H. Lee, J. C. Rasaiah, and J. B. Hubbard, J. Chem. Phys. **85**, 5232 (1986).

[4] S. Senapati and A. Chandra, J. Mol. Struct. THEOCHEM **455**, 1 (1998).

[5] S.-B. Zhu and G. W. Robinson, J. Chem. Phys. **94**, 1403 (1991).

[6] X. Xia and M. Berkowitz, Phys. Rev. Lett. **74**, 3193 (1995).

[7] H. J. C. Berendsen, J. R. Grigera, and T. P. Straatsma, J. Phys. Chem. **91**, 6269 (1987).

[8] J. P. Hansen and I. R. McDonald, *Theory of Simple Liquids* (Academic, London, 1986).

[9] G. M. Torrie, P. G. Kusalik, and G. N. Patey, J. Chem. Phys. **88**, 7826 (1988).

[10] G. M. Torrie, P. G. Kusalik, and G. N. Patey, J. Chem. Phys. **89**, 3285 (1988).

[11] G. Rickayzen and M. J. Grimson, J. Chem. Soc., Faraday Trans. 2 **78**, 893 (1982).

[12] M. S. Wertheim, J. Chem. Phys. **55**, 4291 (1971).

[13] M. Moradi and G. Rickayzen, Mol. Phys. **68**, 903 (1989).

[14] P. Frodl and S. Dietrich, Phys. Rev. A **45**, 7330 (1992).

[15] P. Frodl and S. Dietrich, Phys. Rev. E **48**, 3741 (1993).

[16] S. Nordholm and A. D. J. Haymet, Aust. J. Chem. **33**, 2029 (1980).

[17] M. Johnson and S. Nordholm, J. Chem. Phys. **75**, 1953 (1981).

[18] B. C. Freasier and S. Nordholm, J. Chem. Phys. **79**, 4431 (1983).

[19] S. Nordholm, J. Gibson, and M. A. Hooper, J. Stat. Phys. **28**, 391 (1982).

[20] B. C. Freasier, C. E. Woodward, and S. Nordholm, J. Chem. Phys. **90**, 5657 (1989).

[21] C. E. Woodward and S. Nordholm, Mol. Phys. **60**, 415 (1987); **60**, 441 (1987); J. Phys. Chem. **92**, 497 (1988).

[22] S. Abbas, P. Ahlstrom, and S. Nordholm, Langmuir **14**, 396 (1998).

[23] *Fundamentals of Inhomogeneous Fluids*, edited by D. Handerson (Marcel Dekker, New York, 1992).

[24] L. Mier-y-Teran, S. H. Suh, H. S. White, and H. T. Davis, J. Chem. Phys. **92**, 5087 (1990).

[25] Z. Tang, L. Mier-y-Teran, H. T. Davis, L. E. Scriven, and H. S. White, Mol. Phys. **71**, 369 (1990).

[26] Z. Tang, L. E. Scriven, and H. T. Davis, J. Chem. Phys. **97**, 494 (1992).

[27] C. N. Patra and S. K. Ghosh, Phys. Rev. E **47**, 4088 (1993).

[28] C. N. Patra and S. K. Ghosh, Phys. Rev. E **48**, 1154 (1993).

[29] C. N. Patra and S. K. Ghosh, J. Chem. Phys. **100**, 5219 (1994).

[30] C. N. Patra and S. K. Ghosh, J. Chem. Phys. **106**, 2752 (1997).

[31] J.-H. Yi and S.-C. Kim, J. Chem. Phys. **107**, 8147 (1997).

[32] P. Tarazona, Phys. Rev. A **31**, 2672 (1985); **32**, 3148 (1985).

[33] W. A. Curtin and N. W. Ashcroft, Phys. Rev. A **32**, 2909 (1985).

[34] A. R. Denton and N. W. Ashcroft, Phys. Rev. A **39**, 426 (1989); **44**, 8242 (1991).

[35] J. C. Rasaiah, D. J. Isbister, and G. Stell, Chem. Phys. Lett. **79**, 189 (1981); J. Chem. Phys. **75**, 4707 (1981).

[36] G. V. Vijayadamodar and B. Bagchi, J. Chem. Phys. **95**, 1168 (1991).

[37] C. J. F. Bottcher, *Theory of Electric Polarization* (Elsevier Scientific, Amsterdam, 1985), Vol. 1.

[38] B. Bagchi and A. Chandra, Adv. Chem. Phys. **80**, 1 (1991).

[39] C. G. Grey and K. Gubbins, *Theory of Molecular Fluids* (Clarendon, Oxford, 1984).

[40] J. C. Shelley and G. N. Patey, Mol. Phys. **88**, 385 (1996).